14 From Scattering to Waveguiding: Photonic Crystal Fibres

J. C. Knight, T. A. Birks, R. F. Cregan, J. Broeng, and
P. St. J. Russell

Department of Physics, University of Bath Bath BA2 7AY United Kingdom

Abstract. Photonic crystals are formed of a regularly patterned microstructured material, with a pitch comparable to the optical wavelength. These materials exhibit unusual optical properties due to the interference of the light scattered at the different interfaces, and this has remarkable consequences such as the formation of photonic band gaps. One way of making 2-dimensional photonic crystal materials is to use the technology of optical fibre fabrication. We describe how new optical properties arise in such media, and how they can be used to form novel optical waveguide structures.

1 Introduction

Several existing and developing technologies are capable of producing 2- or 3-dimensionally periodic arrays of scatterers - artificial crystals with a pitch of the order of microns or less. Because in some ways the behaviour of photons in these materials is analogous to that of electrons in naturally-occurring crystals, such microstructured materials have become known as photonic crystal materials [1]. These materials enable new forms of optical elements (waveguides, filters, routers...) and could greatly increase the efficiency and speed of active optical devices. Consequently, they have the potential to have a substantial impact on optics and optoelectronics. The complexity of the interaction of electromagnetic waves with these materials is evidenced by the substantial world-wide research effort in this field over the past decade [2]. Laboratory tests at sub-optical frequencies have demonstrated the validity of the basic theories of electromagnetic waves in these structures, for example demonstrating that there can be ranges of frequency within which light is unable to propagate inside the material. However, the relatively slow progress towards the demonstration of genuine device designs at optical frequencies is a reflection of the several remaining hurdles facing workers in the field. Some of these remaining challenges are: 1) the fabrication of samples with the required pitch, uniformity and refractive index contrast, 2) designing devices in such a way as to avoid the problems due to diffraction of light from 2-dimensionally periodic structures, 3) providing the mechanisms for coupling efficiently into and out of the periodic regions, and 4) comprehensive experimental characterisation of completed samples. This chapter describes an investigation into 2-dimensionally periodic materials being used in the design

F. Moreno and F. González (Eds.): Lectures 1998, LNP 534, pp. 253–267, 2000.

and demonstration of new types of optical fibre waveguide [3–6]. In order to understand the optical properties of the new waveguides it is important to understand the nature of the effects at work in the photonic crystal material which will form the waveguide cladding.

The analogy with the theory of electronic conduction in semiconductors provides a historical framework for our understanding of the interaction of light with a photonic crystal material. Specifically, just as a large number of atoms coupled together in a crystal lattice can give rise to electronic conduction bands and band gaps, so in a 2-dimensional photonic crystal scattering from several surfaces within the material can cause ranges of frequency where electromagnetic propagation is not possible. A large refractive index contrast between the two phases of the microstructured material ensures a significant reflection at each interface, so that only a relatively small number of surfaces are required for strong reflection. This strengthens the effect and makes it possible to find ranges of β - the component of propagation constant perpendicular to the periodic plane - for which there is a complete photonic band gap, independent of direction with respect to the crystal lattice [7]. Within this range of β there are no propagating modes, and the only allowed electromagnetic fields are evanescent. This suggests that the optical properties of photonic crystal materials can be modelled as a multiple-scattering problem[8], where the number of scatterers which one needs to consider might be relatively large but remains finite. It further suggests that scattering studies would be a fruitful way of investigating the optical properties of these microstructured samples.

2 Scattering in Periodically Microstructured Materials

Previous treatments of multiple scattering by cylinders or more usually spheres have concentrated on the scattering by a few particles which are arrayed in an irregular fashion, and which are illuminated from free space [9,10]. Convergent solutions have been obtained, and evaluated numerically for many simple configurations. Simple experiments have been performed to verify the performance of the scattering algorithms [11,12]. Such algorithms have several drawbacks as far as the present work is concerned: they converge extremely slowly for the relatively large number of scatterers involved in the scattering process and they do not take advantage of the periodic nature of the material structure to optimise the calculations. On the other hand the methods originally developed for studying the scattering of x-rays in naturally-occurring crystals have much to recommend them: the use of inverse-space diagrams (k-vector diagrams) lends itself naturally to the solution of problems involving periodic materials. Much has been made of the series of methods derived from the analysis of electronic properties of naturally-occurring crystals, the plane-wave method in particular [13]. Although these methods are admirably suited to the numerical analysis of continuous periodic materials they

do not in themselves provide solutions to the scattering problem, in which the interface with the modes of free space are of prime importance. "Scattering" in this context can be applied to two rather different situations: in a conventional sense (when the microstructured material is illuminated from free space by a propagating beam) and in a rather different sense where the interaction of the material itself with a time-harmonic electromagnetic field is modelled as being due to a continuous process of multiple scattering (e.g. using a Green's function approach). In working towards our objective of waveguiding in a microstructured material by a photonic band gap effect, the second of these is the fundamental effect which we are interested in, while the first promises to be a useful characterisation tool in assessing our progress towards that goal.

The waveguides to be discussed here are made by forming the required 2-dimensionally periodic structure on a macroscopic scale in the form of a preform, and then reducing the cross-sectional scale of the structure by several orders of magnitude by drawing this preform down into a fine fibre on a fibre-drawing tower at an elevated temperature. The preform is made by stacking together in a close-packed arrangement hundreds of silica tubes and rods, each of which is typically 0.75 mm in diameter and 40 cm in length. The preform is then of the same length and perhaps 15 mm in diameter, while the final fibre into which the preform is drawn - which can be many kilometres in length - has a diameter in the range of $30 - 200$ μm. Careful adjustment of the temperature at which the fibre is drawn allows one to maintain the periodic pattern of air holes in the cross-section of the final fibre, where the pitch of the "crystal lattice" is of the order of microns. The air holes , which can be as small as 50 nm in diameter, run down the entire length of fibre, giving an aspect ratio of the order of 10^9. A schematic representation of a fibre, which we call a photonic crystal fibre (PCF), is shown in Fig. 1.

Photonic crystal fibre differs from all other 2d photonic crystal materials in that it can be made in virtually limitless lengths. This is a major departure: it means that PCF represents a truly three-dimensional material, with a periodic patterning in two of these dimensions. Thus in PCF we have the opportunity to investigate a two-dimensionally periodic material without in any way restricting interest to the periodic plane. One result of this is that it is possible to obtain band gaps for relatively small values of refractive index contrast - in-plane band gaps are not possible for the silica/air material system being described here. This is due to the greater reflection at each interface which occurs for out-of-plane incidence - we have taken this effect to an extreme case in demonstrating photonic band gap effects in a honeycomb lattice structure, as described in Sect. 6. A second result of the three-dimensional nature of the fibre is that PCF represents an ideal way to fabricate useful photonic crystal devices for a three-dimensional world. Our major interest in this type of structures is exactly this: we aim to design, fabricate and demonstrate waveguiding optical fibres which are completely

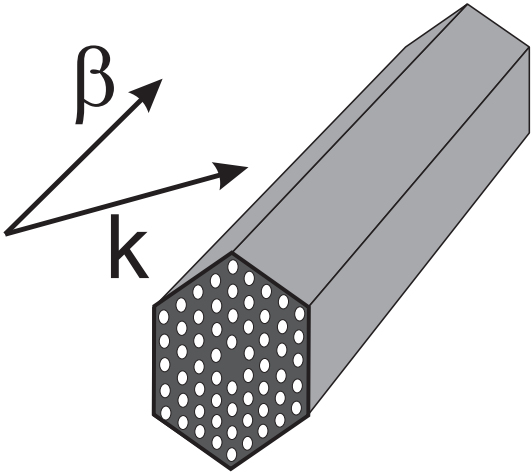

Fig. 1. Schematic representation of a photonic crystal fibre. The arrows indicate the component β of the wavevector k which is parallel to the fibre axis.

different to conventional waveguides. Instead of using existing materials with different refractive indices to define the waveguiding structure, we have engineered new microstructured materials which have the desired properties.

3 Scattering from Photonic Crystal Fibres

Our interest in the scattering properties of photonic crystal fibres lies in the use of scattering patterns as an indicator of the band structure of the photonic crystal - not so much the common scattering processes (such as Fraunhofer or anomalous diffraction), but the multiple scattering process that takes place within the microstructured fibre. Thus, it is important that we investigate a suitable range of incident propagation constants - side-illumination of the fibre from air even at grazing-incidence (i.e. beam direction parallel to the fibre axis) can only give a maximum β-value of the free-space wavevector [14,15]. However, our samples have an inter-hole spacing substantially greater than $\lambda/2n$, so that the fundamental Bragg conditions lie beyond the critical angle for a silica/air interface. In order to access higher wavevectors β than k we have embedded fibre samples in an oil with a refractive index close to that of silica ($n_s = 1.45$), thus enabling β-values up to $n_s k$ for oblique illumination. This is done by mounting the fibre sample as shown in Fig. 2.

A short length of fibre (typically 25 mm) is stoppered at both ends using glue and is mounted along the axis of a cylindrical cell, which is fitted with transparent windows at both ends. The cell is placed horizontally on rotation stages enabling it to be rotated about its own axis and also to be rotated in the horizontal plane. The fibre is then illuminated with a focussed laser

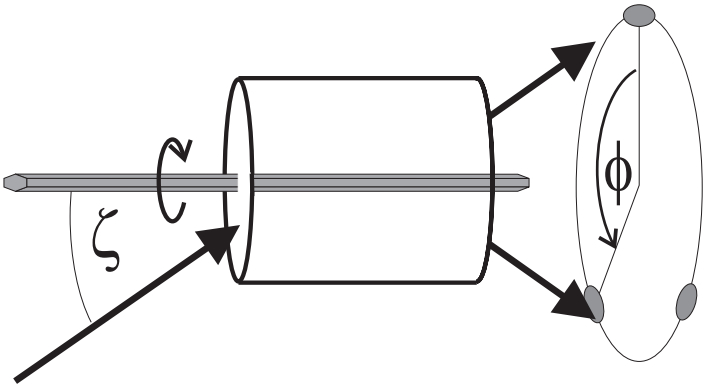

Fig. 2. Schematic diagram showing the experimental configuration used to record scattering patterns. Focussed light incident from the left enters the silica cell, and scatters off the photonic crystal fibre. The scattered cone of light falls onto a screen on the right hand side of the diagram, which is imaged onto a vidicon camera. The angle ζ, and the orientation of the fibre about its own axis, can be varied. The unscattered light falls on the screen at $\phi = 0$

beam ($\lambda = 1.5$ μm, $NA = 0.008$) through one of the end windows, and the scattered light passes through the other window before falling onto a screen. Illumination at a single angle ζ thus gives rise to scattering into a cone, which appears as a ring on the screen [16]. This screen is imaged onto a vidicon camera and the video signal from the camera is acquired using a frame-grabber, enabling the acquisition of all the main features of the entire scattering pattern of a fibre at a particular angle ζ.

For small air holes (as shown in Fig. 3), the object can be modelled as a coherent array of Rayleigh scatterers embedded in a silica matrix, giving rise to Bragg scattering at particular angles of incidence.

Assuming the first Born approximation, the angular width of the Bragg peaks is determined roughly by the number of scatterers involved in the process. Because the silica matrix is index-matched to the oil in our experiment, there is virtually no scattering from the surface of the fibre in this case. Thus, the scattering is characterised by sharp features appearing for particular angles ζ, with very little scattering at other angles. Most of the light passes through the sample without being scattered, at all incident angles. An example of a scattering pattern observed from a fibre with a triangular array of small air holes (with diameter $d < 0.2$ μm spaced by $\Lambda = 2.2$ μm) is shown in Fig. 4. The incident angle has been adjusted so as to coincide with one of the Bragg points of the fibre. The unscattered light causes the bright spot at $\phi = 0°$. The Bragg scattering angles for a fibre with a particular lattice type and pitch are readily predicted using the inverse lattice and the Brillouin zone boundaries. In Fig. 4b the filled circles show the array of inverse lattice points for the triangular lattice, while the broken lines show the Brillouin

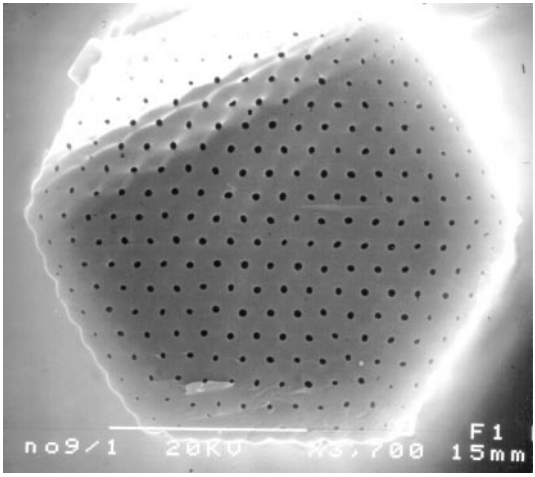

Fig. 3. A scanning electron micrograph of a PCF with small air holes, as used to observe Bragg scattering patterns. The fibre shown has a pitch of 1.3 μm

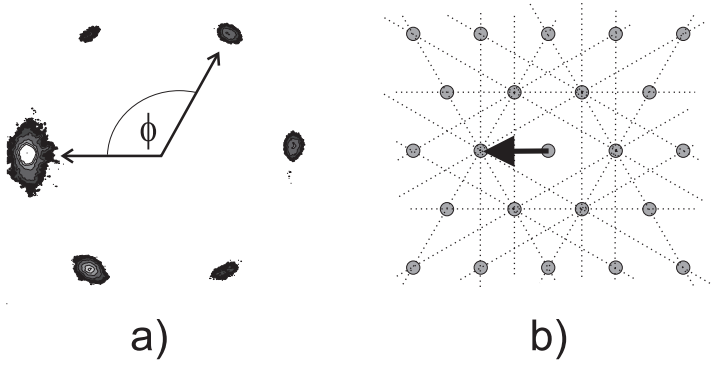

Fig. 4. (a)shows a scattering pattern observed from a fibre such as that in figure 3 excited at one of the Bragg conditions. The unscattered light is on the left at $\phi = 0$. **(b)** shows the Brillouin zone diagram for the triangular lattice. The Brillouin zone boundaries are indicated by dotted lines. A heavy arrow shows the incident k-vector used to excite the Bragg condition in **(a)**

zone edges. To predict the Bragg scattering points, one draws an arrow from the origin in the direction corresponding to the direction of incidence on the crystal. The arrow represents the incident in-plane wavevector, so the length of the arrow is simply k_T. If the tip of the arrow falls on a Brillouin zone boundary, Bragg scattering will occur. The directions of this scattering can be predicted from the directions of the Brillouin zone edges at this point. In the example shown (Fig. 4a) the light is incident along the $\Gamma - X$ direction

and at an angle which corresponds to the arrow shown in Fig. 4b, giving rise to the attractive and highly symmetrical scattering pattern shown.

A significantly more complicated situation can arise when the size of the air holes increases so that they become substantial. In this case each air hole can no longer be approximated as a Rayleigh scatterer, while the significant volume of scatterers in the medium results in a rapid attenuation of the field as the light moves through the crystal at some angles. Furthermore, there is substantial scattering at the interface between the index-matching oil (which has the index of pure silica) and the fibre (which has, effectively, a lower refractive index).This last difficulty is compounded by the fact that the fibre has a hexagonal external surface (see Fig. 3), so that more than one interface is involved for any angle of incidence. These effects give rise to intricate scattering patterns with very different general features to those observed from small-air-hole samples. Specifically, strong scattering features are observed at all angles of incidence, in contrast to the sharp angular features observed from the small air-hole fibre. As in the small air-hole case, the patterns are dominated by a few strong and symmetrically-positioned peaks. Unlike the small air hole case, however, the patterns are heavily weighted in the backward direction, and we attribute this to the failure of the first Born approximation.

To understand the observed scattering patterns we need to know something about the possible modes within the photonic crystal material, and how these will be excited in our experiment. In any air-silica fibre, there is a maximum attainable value of β - the largest propagation constant possible parallel to the fibre axis. We refer to this as the propagation constant of the fundamental space-filling mode, β_{fsm}. The modal index β_{fsm}/k associated with this mode of propagation must be below that of pure silica, although it can approach that of silica for very small air holes and for short wavelengths. Numerically, the propagation constant of this mode can be readily estimated[4]. As a result of this maximum β-value the liquid/fibre interface can support total internal reflection for sufficiently small angles of incidence from the liquid side. At such small angles we expect that the fibre will then act as a perfect reflector. Knowing the value of β_{fsm} allows us to calculate the critical angle for the oil/fibre interface. The scattering pattern in Fig. 5 was recorded for incidence along the $\Gamma - J$ direction at just beyond the critical angle, and shows a small amount of unscattered light (at $\phi = 0°$) and two bright spots at 120° from the forward direction. These two bright spots correspond to the simple total reflection from the effective refractive index interface at the fibre surface (see figure inset). These occur for a range of angles from the smallest experimentally attainable up to a maximum angle of about $\zeta = 8.5°$ where other features start to appear in the scattering diagram. The maximum angle at which the scattering patterns can be explained by simple reflections from the external surface is in excellent agreement with the critical angle calculated from the computed value of β_{fsm}.

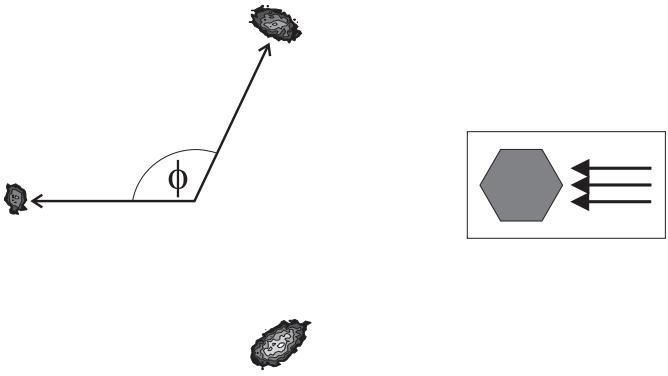

Fig. 5. Scattering pattern observed from a large-air-hole fibre sample at a small angle ζ (large β-value). The incident β is greater than the β_{fsm} for the structure, so that the scattering pattern is simply due to reflection from the external surfaces, as shown in the inset on the right

At larger angles of incidence we expect to see complex scattering patterns due to imperfect mode-matching at the fibre surface, while in certain discrete angular ranges (when we have chosen a β-value corresponding to a band gap of the microstructured material) we expect simple patterns very similar to that in Fig. 5. The observed scattering patterns do indeed show the appearance of more complicated features at angles slightly larger than that used in recording Fig. 5. These more complex scattering patterns result from partial mode coupling at the fibre surface under conditions where there are some allowed modes within the fibre. We have yet to see clear evidence in the scattering patterns of a complete photonic band gap, even in those samples where theory predicts that such a gap should occur. We believe that this is due to the departures from perfect periodicity in the fibre structure close to the external surfaces. We plan to concentrate our future studies on those fibres where we have direct experimental evidence for the existence of a band gap (see Sect. 6, and where electron microscopy shows that the fibre structure maintains its periodicity right to the external surface of the fibre.

4 Design and Fabrication of Photonic Crystal Fibre Waveguides

In order to use photonic crystal fibre as the cladding of an optical waveguide we need to use the periodic material under one of the two circumstances when we can expect to find total reflection from the structure, viz. incidence upon the structure with a β-value above the largest possible β in the periodic material ($\beta > \beta_{fsm}$ - see Sect. 5), or incidence with a β-value corresponding to a band gap of the periodic material. The first condition can only be satisfied if the waveguiding core is formed by a "high-index" defect within the structure

- a region containing a reduced amount of low-index material. This is most readily realised by replacing a single one of the capillaries in the stacking process with a solid cane of similar external diameter - we refer to this type of fibre as "index-guiding", as the guidance mechanism is in many ways similar to that in conventional optical waveguides. On the other hand, "band gap" waveguiding is possible even when the crystal defect comprises an extra air hole (a "low-index defect"), and using just such a defect to demonstrate the effect has the advantage that the index-guiding mechanism can be excluded. In the next two sections we describe briefly the main observed features of these two types of guidance.

5 Waveguiding by Total Internal Reflection from an Effective Index Structure

A scanning electron micrograph showing an example of part of a cross-section through an index-guiding fibre structure is shown in Fig. 6.

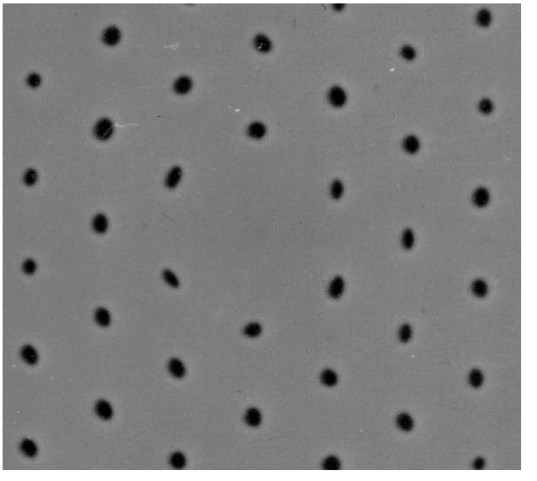

Fig. 6. Portion of the cleaved face of an index-guiding photonic crystal fibre. The site of the missing air hole constitutes a "high-index defect" in the photonic crystal lattice, causing the appearance of trapped modes localised within this region. The guided modes have propagation constants β greater than the largest value of propagation constant found in the periodic region β_{fsm}, and can thus be considered to arise as a result of total internal reflection from the silica/air structure.

The fibre shown is typical of those which we have studied. The parameters of the fibre are $\Lambda = 2.3$ μm and air hole size $D = 400$ nm. Our observations of the waveguiding properties of the fibre shown in Fig. 6 are that the fibre supports a guided mode which is confined to the vicinity of the "high-index"

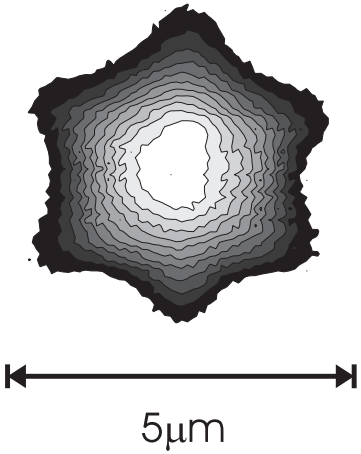

Fig. 7. Modal intensity pattern recorded at a cleaved output face of an index-guiding photonic crystal fibre. The light intensity peaks in the centre of the "lattice defect" site which has the missing air hole, and has deep minima at the positions of the nearest air holes.

defect in the structure. The observed modal intensity pattern observed for a wavelength of $\lambda = 633$ nm is shown as a contour plot in Fig. 7. The guided mode is seen to be tightly confined to the vicinity of the defect and to be structured so as to avoid the nearest air holes. The guided mode pattern is independent of the way in which the light is coupled in to the fibre, and of any bends and twists in the fibre length: the observed modal profile is that of the fundamental guided mode, and no other confined modes are excited. Very similar patterns to that shown in Fig. 7 are observed at all excitation wavelengths between $\lambda = 1.5$ μm and $\lambda = 337$ nm, a variation in wavelength of a factor of more than 4. Likewise, by making fibres similar to that in Fig. 6 but with a different scale (up to a factor of 5 larger) we find that there is but a single robust guided mode. Such behaviour is quite different to that observed in conventional fibres, where increasing the core diameter or decreasing the wavelength by more than a factor of 2 will introduce higher-order guided modes. For very long wavelengths ($\lambda >> \Lambda$) the behaviour of our fibre is expected to approach that of a conventional optical fibre with a core refractive index equal to that of silica and a cladding index equal to the root-mean-square volume-weighted index of the silica/air structure. For shorter wavelengths, the morphological microstructure of the fibre cladding results in a microstructuring of the optical fields within the cladding. As a result, the apparent optical properties of the cladding change as a function of wavelength (or, more correctly, as a function of Λ/λ). This variation in the "effective refractive index" [4] is closely related to our observation that the fibre can be "endlessly single-mode", not supporting a second bound mode for any wavelength no matter how short. Likewise, other observed properties

of the fibre are different to those familiar from conventional waveguides. For example, the bend loss characteristics and the dispersion [17] of the fibre are quite different from those in normal optical fibres, especially in the regime where a conventional fibre would be overmoded.

6 Band Gap Waveguiding

Although it is possible (at least in principle) to form an optical waveguide by using the band gap formed by a triangular array of air holes as a cladding material, we have not yet observed such guidance. This can be attributed in part to the difficulty of fabricating samples with a sufficiently high degree of uniformity which have a small enough pitch Λ and large enough air holes D. However, we have observed a closely related type of waveguiding, due to a photonic band gap in a honeycomb lattice. The requirements for uniformity are relaxed in this case because the honeycomb structure has intrinsically broader band gaps [18]. This is especially true for substantially out-of-plane propagation [19]. An electron micrograph showing such a fibre is presented in Fig. 8. This fibre was fabricated by drawing down a stack formed from

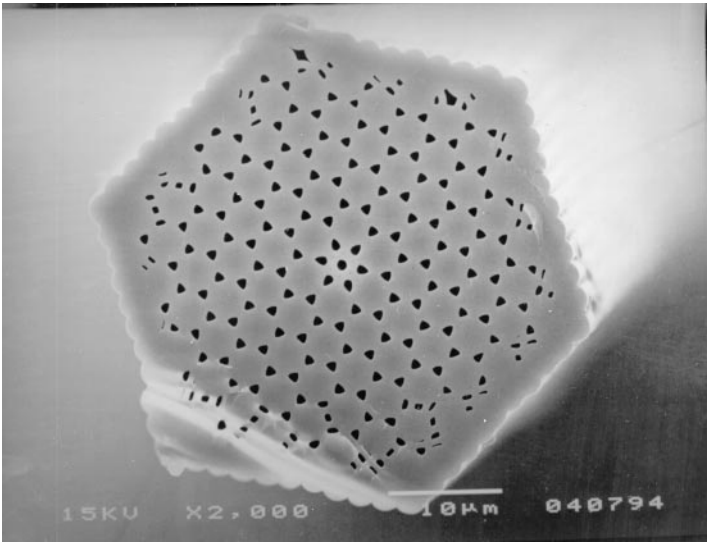

Fig. 8. Scanning electron micrograph showing a honeycomb "band gap" fibre. In this structure, light becomes trapped in the vicinity of the extra air hole in the centre of the fibre (a "low-index defect"). The confinement in this case is due to the band gap of the surrounding band-gap material, not total internal reflection.

solid silica canes as well as hollow capillaries. An extra air hole in the middle of the stack forms a region with an increased air fraction - a "low-index"

defect in the honeycomb lattice. Instead of a honeycomb lattice of air holes the fibre shown in 8 can be usefully considered to be a triangular array of almost close-packed silica rods. Each of these rods would, if isolated, support waveguide modes with distinct values of propagation constant. When a large number of these are coupled together, each mode splits into a large number of closely-spaced modes, leading to transmission bands through the material. However, the composite material can also have regions of β where no modes exist. For our samples, numerical modelling [19] predicts the appearance of such band gaps at visible frequencies. By introducing a low-index defect into the structure, we can create localised modes - confined modes which are trapped to the vicinity of the defect by the band gap of the surrounding material. It should be noted that the band gaps which we have been study-

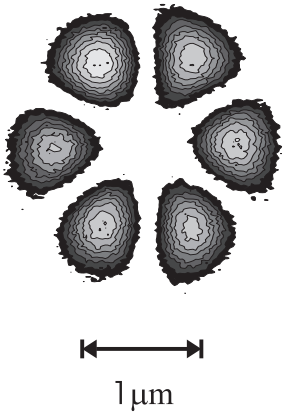

Fig. 9. Near-field intensity map observed from a defect-guided mode in a honeycomb band-gap fibre, such as that shown in figure 8. The mode has been excited using a laser source (λ = 528 nm). The six symmetric lobes appear around the central "defect" hole in the honeycomb structure(see Fig. 8. The corresponding far-field pattern (not shown) has a zero on the axis, indicating the presence of phase reversals in the guided mode profile.

ing in the honeycomb structure as shown in Fig. 8 differ from those formed in a triangular lattice in an important respect: band gaps in the triangular structure arises from a strengthening of Bragg scattering [7], and as such can potentially appear over a very broad range of β. The "coupled resonator" model [7] outlined above for the honeycomb band gap suggests that the gaps in this structure will appear for relatively large values of β. Indeed, for such large values of β propagation is in general forbidden within the material, light being evanescent in the air gaps. Propagating modes in this regime only arise at specific β-values corresponding to resonances of the individual silica strands, which when coupled together form "band windows" within the broad

forbidden region. Thus, band gaps are likely to be broader and intrinsically more stable than those formed in a triangular structure for smaller β-values. While there is no evidence that low-β Bragg-type band gaps cannot appear in a honeycomb structure, there is at present no reason to believe that these could be more easily observed than in a triangular lattice. Bragg-type band gaps in a photonic crystal fibre are an especially attractive goal because it is possible (at least in principle) to use such band gaps to form waveguides in which the guided mode is trapped within an air hole. Naturally, to form this mode would require a band gap with a relatively low value of β. Such a waveguide would have obvious applications. Nonetheless, the "coupled resonator" band gaps can be used to form confined modes within a honeycomb structure, and these can be observed at low-index defect sites such as that in Fig. 8. An example of such a guided mode is shown in Fig. 9. The guided mode field profile has variations on the scale of approximately 1 μm, far sharper than those observed in the high-index defect guiding fibre. This indicates a faster phase variation in the periodic plane than in the index-guiding case, which is directly related to the smaller value of out-of-plane propagation constant β in the present mode. The modal field pattern looks distinctly like a higher-order mode of the fibre core, and indeed one can think of it as such. Lower modes (with larger values of β) will exist, but they will not be confined to the vicinity of the core by the cladding material as they fall outside the band gap. The guided mode shown in Fig. 9 is confined to the defect only for a relatively narrow range of frequencies - it is confined for wavelengths between 458 nm (blue) and 528 nm (green) but is not confined at 633 nm (red). This strong spectral dependence means that very beautiful and brightly coloured modal field patterns can be observed in these structures using a white light source [6].

7 Conclusions

We have adapted the technology of optical fibre fabrication to produce two-dimensionally periodic silica/air photonic crystal materials. These materials consist of fine fibres with a regular and 2-dimensionally periodic array of air holes running down their length. These air holes can have diameters of less than 100 nm and be spaced by distances of the order of 1 μm or greater. The optical properties of these microstructured materials are quite different from those of silica, and can usefully be studied by scattering experiments. These new properties have enabled us to observe waveguiding within the photonic crystal fibres by introducing purposeful defects into the photonic crystal lattice. These photonic crystal fibre waveguides have some startling properties, and there is a great depth of work still to be done both in understanding those effects which have been observed, and in extending the limits of what is technologically achievable so as to observe new effects.

8 Acknowledgements

This work was funded by the U.K. Engineering and Physical Sciences Research Council and by the D.E.R.A., Malvern, U.K. T. A. Birks is a Royal Society Research Fellow. J. Broeng also works at the Center for Communications, Optics, and Materials, Technical University of Denmark, DK2800 Lyngby, Denmark. J. C. Knight is grateful to the organisers of the Cursos de Verano de Laredo for the opportunity to present this work at a Summer School.

References

1. Joannopoulos, J. D., Meade, R. D., Winn, J. N, (1995) Photonic crystals: molding the flow of light, Princeton University Press, Princeton, N.J.
2. See e.g. the special issues of Journ. Opt. Soc. Am. B 10, 279-413, edited by C. M. Bowden, J. P. Dowling and H. O. Everitt (1993), J. Mod. Opt. 41, 2 edited by G. Kurizki and J. W. Haus (1994) and Microcavities and Photonic Bandgaps: Physics and Applications, J. G. Rarity and C. Weisbuch, eds. (Kluwer, Dordrecht, 1996)
3. Knight, J. C., Birks, T. A., Russell, P. St. J., and Atkin,D. M., (1996) All-silica single-mode optical fiber with photonic crystal cladding. Opt. Lett. **21** 1547–1549 (1996)
4. Birks,T. A., Knight J. C., and Russell, P. St. J., (1997) Endlessly single-mode photonic crystal fibre. Opt. Lett. **22** 961-963
5. Birks, T. A., Roberts, P. J., Russell,P. St. J., Atkin, D. M., Shepherd, T. J. (1995) Elect. Lett. **31**, 1941
6. Knight J. C., Broeng,J., Birks, T. A. and Russell, P. St. J. (1998) Photonic Band Gap guidance in optical fibers. Science 282 1476
7. Russell, P. St. J., Birks, T. A., and Lloyd-Lucas, F. D., (1995) Photonic Bloch Waves and Photonic Band Gaps (Confined Electrons and Photons: New Physics and Applications, E. Burstein and C. Weisbuch, eds.) Plenum, New York
8. Li, L. M, Zhang, Z. Q. (1998) Multiple-scattering approach to finite-sized photonic band-gap. Phys. Rev. B **58** 9587-9590
9. Fuller, K. and Kattawar, G. W. (1988) Consummate solution to the problem of classical electromagnetic scattering by an ensemble of spheres. I: Clusters of arbitrary configuration. Opt. Lett. **13**, 1063-1065
10. Tsuei, T.-G. and Barber, P. W. (1988) Multiple scattering by two parallel dielectric cylinders. Appl. Opt. **27** 3375-3381
11. Arnold S., Ghaemi A., Hendrie P., Fuller, K. A., (1994) Morphological Resonances Detected From A Cluster Of 2 Microspheres Opt. Lett. **19** 156-158
12. Schlicht, B., Wall, K. F. Chang, R. K. and Barber, P. W. (1987) Light scattering by two parallel glass fibers. Journ. Opt. Soc. Am. A **4**, 800–808
13. Ho, K. M., Chan, C. T., Soukoulis, C. M., (1990) Existence of a photonic gap in periodic dielectric structures. Phys. Rev. Lett. **65** 3152-3155
14. Knight, J. C., Birks, T. A., Russell, P. St. J., and Rarity, J. G. (1998) Bragg scattering from an obliquely-illuminated photonic crystal fibre. Appl. Opt., **37** 449–452

15. Cregan, R. F, Knight, J. C., Russell, P. St. J., Roberts, P. J. (1999)Scattering by Photonic Crystal Fibres. To be submitted.
16. Bohren, C. F., and Huffman, D. R. (1983) Absorption and Scattering of Light by Small Particles. Wiley-Interscience, New York
17. Gander, M. J., McBride, R., Jones, J. D. C., Mogilevtsev, D. Birks, T. A., Knight, J. C., and Russell,P. St. J. (1999) Experimental measurement of group velocity dispersion in photonic crystal fibre. Electron. Lett. **35**, 63–64
18. Cassagne, D., Jouanin, C., Bertho, D. (1996) Hexagonal photonic-band-gap structures. Phys. Rev. B **53**, 7134
19. Broeng, J., Barkou, S. E., Bjarklev, A., Knight, J. C., Birks, T. A. Russell, P. St. J. (1998) Highly increased photonic band gaps in silica/air structures. Optics Comm. **156** 240-244